Time-Resolved Study of Luminescence in $LiGd_{1-x}F_4:Eu^{3+}{}_x$

Nobuyuki Takeuchi, Shinngo Ishida, Arima Matsumura, and Yo-ichi Ishikawa*

Department of Chemistry and Materials Technology, Kyoto Institute of Technology, Matsugasaki, Sakyo-ku, Kyoto 606-8585, Japan

Received: December 31, 2003

Radiative and energy-transfer processes in $LiGd_{1-x}F_4:Eu^{3+}{}_x$, where the ground state of $Gd^{3+}(^8S_{7/2})$ was selectively excited to the ^6I_J state by a 275-nm pulsed laser irradiation, were studied by time-resolved luminescence spectroscopy. Two decay components were observed in $Gd^{3+}:{}^6P_{7/2} \rightarrow {}^8S_{7/2}$ emission at 313 nm. One was influenced by the Eu^{3+} addition, and the other was not. The Eu^{3+}-sensitive decay rate increased up to ~1.0 mol % and then remained almost constant up to 10 mol % Eu^{3+}. The Eu^{3+}-insensitive decay had a rate of about 7×10^2 s^{-1} ($\tau \approx 1.5$ ms). The intrarelaxation rate of the ^6I_J state to the luminescent $^6P_{7/2}$ state of the Gd^{3+} ion was estimated to be about 1.3×10^5 s^{-1} from the rise of the 313-nm luminescence ($\tau_{rise} \approx 8$ μs). This rate was almost independent of the Eu^{3+} concentration. The luminescence intensity from Eu^{3+} at around 591 nm and at 613 nm monotonically increased with increasing Eu^{3+} concentration up to 1.0 mol % Eu^{3+}, above which it remained constant. This implies the absence of more efficient energy transfer from Gd^{3+} to Eu^{3+} at higher Eu^{3+} concentration. The emission lifetime of the $^5D_0$ state of Eu^{3+} ion was estimated to be about 8 ms.

1. Introduction

The absorption and emission properties of crystalline $LiGd_{1-x}F_4:Eu^{3+}{}_x$ are very similar to those of the free ions, Gd^{3+} and Eu^{3+}, despite any interaction of the ions through chemical bonding. The similarity of the electronic energy level diagrams to those of the free ions, narrow spectral width, long lifetime, and low transition probabilities are interpreted in terms of the shielding of 4f electrons from the electric field of surrounding ions by the $6s^2$ electrons. Such a specific arrangement of relatively unperturbed emissive rare-earth ions gives a chance to investigate electronic energy transfer between two ions, donor−acceptor, separated at a discrete distance.

Systems of two kinds of trivalent rare-earth ions, one acting a donor and the other as an acceptor, have been used for the study of the electronic energy transfer in the solid phase.[1−4] In these studies, an amorphous material was mainly applied as the host matrix to provide a homogeneous distribution of the ions. The analysis of the experimental data was based on the resonance transfer of electronic excitation energy mechanisms such as electronic multipole interaction (Förster model) or exchange interaction (Dexter model). In the crystalline phase, a fast energy-transfer rate of 2×10^{11} s^{-1} was estimated for the shortest $Gd^{3+}-Gd^{3+}$ separation (3.557 Å) in a one-dimensional Gd^{3+} compound, $Ca_4GdO(O_3)_3$.[5] If such a fast energy migration plays an important role in the energy-relaxation processes in the solid phase, the transient profile of the donor emission curves may not be treated by a theoretical single-step resonance energy transfer.

An interesting phenomenon of visible quantum cutting was recently reported for the Gd^{3+}(donor)/Eu^{3+}(acceptor) system in $LiGd_{1-x}F_4:Eu^{3+}{}_x$ crystals.[6−9] One of the important applications of this study has been to develop a vacuum ultraviolet (VUV) downconverter for high-efficiency mercury-free fluorescence lamps.[10] When a $Gd^{3+}(^8S_{7/2})$ ion is excited by VUV light at 202 nm, the accessible excited states of Gd^{3+} with $4f^7$ configuration (^6G_J) are thought to have a relatively long emission lifetime. Efficient energy transfer to an acceptor ion, Eu^{3+}, without phonon excitation of the lattice is required for an efficient visible luminescent system. It is important to study the energy-transfer dynamics as well as the spectral and energetic properties for understanding of the visible luminescence of those materials following VUV or UV excitation.

In this study, we measured the transient behavior of the luminescence from Gd^{3+} and Eu^{3+} ions in $LiGd_{1-x}F_4:Eu^{3+}{}_x$ when Gd^{3+} ($^8S_{7/2}$) was excited selectively to Gd^{3+} (^6I_J) by a 275-nm pulse laser irradiation, aiming at elucidating kinetically the intrarelaxation and the electronic energy-transfer rates between excited state of Gd^{3+} and ground state of Eu^{3+}. The variation of the Eu^{3+} content for the kinetic study did not change the lattice constants of the scheelite structure because of the similarity of the ionic radius between Gd^{3+} (0.938 Å) and Eu^{3+} (0.950 Å),[11] allowing us to observe the electronic energy transfer between donor (Gd^{3+}) and acceptor (Eu^{3+}) separated at a fixed distance determined by the crystalline structure.

2. Experimental Section

A stoichiometric quantity of LiF (99.9%, Wako), GdF_3 (99.5%, Wako), and EuF_3 (99.9%, Wako) was thoroughly mixed in an alumina mortar. The mixture was pressed in a disk and fired under an N_2 atmosphere at 550 °C for 1 h. The heating rate to 550 °C was about 5 °C min^{-1}, and the cooling rate to room temperature was about −5 °C min^{-1}. The fired disk was ground to a powder, re-pressed into a disk, and re-fired in a manner similar to the first firing. The formation of the $LiGd_{1-x}F_4:Eu^{3+}{}_x$ phase was proven by XRD analysis with a Rint-2000 diffractometer as shown in Figure 1. $LiGdF_4$ and $LiEuF_4$ are reported to have the scheelite structure.[12] As the lattice constants of $LiGdF_4$ (5.219 Å × 10.97 Å) were very similar to those of $LiEuF_4$ (5.228 Å × 11.03 Å), the variation

* To whom correspondence may be addressed. E-mail: ishikawa@ipc.kit.ac.jp.

10.1021/jp031345h CCC: $27.50 © 2004 American Chemical Society
Published on Web 07/22/2004

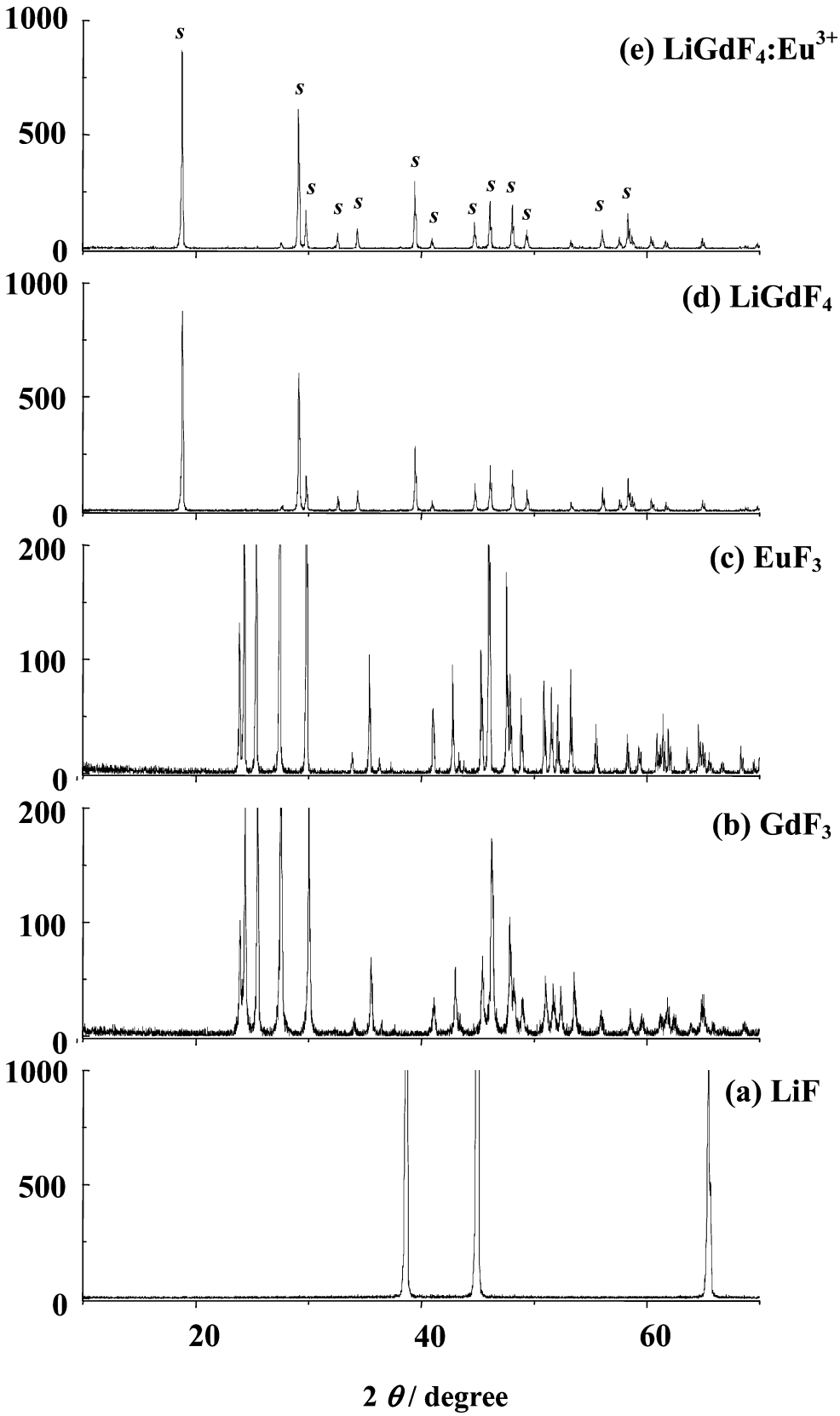

Figure 1. XRD patterns of $LiGdF_4:Eu^{3+}$ and related crystals (a) LiF, (b) GdF_3, (c) EuF_3, (d) $LiGdF_4$, and (e) $LiGdF_4:Eu^{3+}$ (10 mol % Eu^{3+}). The peaks corresponding to the Joint Committee on Powder Diffraction Standards data are denoted by "*s*".

could not be observed in the XRD patterns of $LiGd_{1-x}F_4:Eu^{3+}{}_x$ when the contents of Eu^{3+} were changed by a little. Figure 2 shows the effect of Eu^{3+} ion addition on the lattice constants (*a* and *c*), as estimated by the least-squares method from the X-ray diffraction spectra of our $LiGd_{1-x}F_4:Eu^{3+}{}_x$ crystalline powders synthesized by the above-mentioned procedure. The linear relation might support the substituted solid solution on the basis of Vegard's rule.[13] The resultant powder was pressed in a disk ($\phi \approx 20$ mm, $t \approx 3$ mm) for spectroscopic measurement using a JASCO FP-6500 spectrofluorimeter. The resolution was

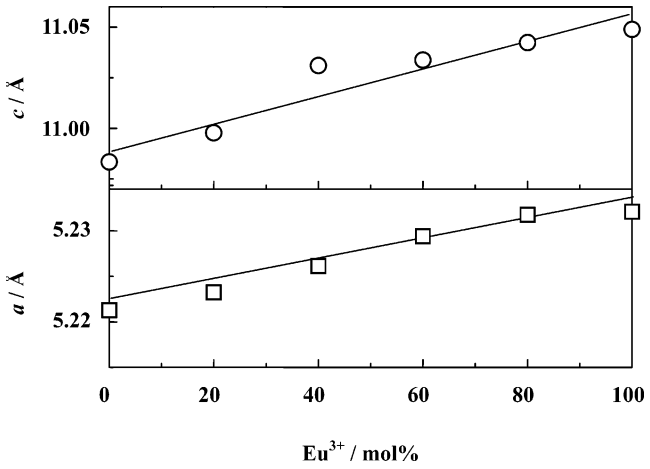

Figure 2. Eu^{3+} ion concentration effect on the lattice constants (*a* and *c*) of $LiGd_{1-x}F_4:Eu^{3+}$ crystals. Both lattice constants show the linear dependence on the Eu^{3+} concentration, supporting the substituted solid solution.

1 nm for both emission and excitation spectra. The excitation bandwidth for emission spectra was 5 nm. The emission collection slit function was 5 nm for the excitation measurements.

A pulsed OPO laser system with a frequency-doubling option (Spectra-Physics MOPO 730/FDO) excited by a pulsed Nd:YAG laser (Spectra-Physics GCR-290-10) was used for a 275-nm pulse radiation with the repetition rate of 10 Hz. The laser pulse had a width of less than 8 ns (fwhm) and the energy of about 50 μJ pulse^{-1}. The output luminescence signal was detected by a photomultiplier (Hamamatsu R-928) set behind the exit slit of monochromator (Spex Minimate, $f = 20$ cm, $\Delta\lambda = 10$ nm) and was subsequently sent to a digital oscilloscope (Tektronix TDS 320). The digitized output was stored and analyzed by a personal computer. The typical average number of emission waveforms was 256. All measurements were carried out at room temperature.

3. Results and Discussion

Emission and excitation spectroscopic measurements were carried out before the time-resolved emission measurements. Figure 3 shows the UV/vis emission spectra of $LiGd_{1-x}F_4:Eu^{3+}{}_x$ excited at 275 nm corresponding to the $^6I_J \leftarrow {}^8S_{7/2}$ transition of Gd^{3+}. Some emission lines besides the strong bands at around 313 nm and 580−620 nm were observed in the region between 400 and 580 nm. These emission lines were assigned to the transitions of $^5D_{3-1} \rightarrow {}^7F_J$ from the known energy levels of Eu^{3+} in $LaCl_3$.[14] The fact that these emission intensities monotonically increased with increasing Eu^{3+} concentration supported the assignment. Such emissions from spin−orbit states higher than $^5D_0$ of Eu^{3+} were not observed in the case of soda-lime silicate glasses codoped with Gd^{3+} and Eu^{3+},[15] showing that the internal relaxation in Eu^{3+} is slower in the crystal than in the glass and/or the transition probability is higher in the crystal. The weak emission lines attributed to Eu^{3+} in $LiGdF_4$ without added Eu^{3+} suggested that the Eu^{3+} ions were present as impurities in the GdF_3 starting materials. The emission intensity of Gd^{3+} at 313 nm decreases by increasing the Eu^{3+} concentration but does not completely disappear. That of Eu^{3+} at 591 nm increases up to ∼1.0 mol % Eu^{3+} addition and then remains constant until 10 mol % Eu^{3+} addition (Figure 4). There seems to be two differences from the case of glass.[15] First, in the glass, the emission of Gd^{3+} completely disappears even at 1.0 mol % Eu^{3+} addition, and second, the emission of Eu^{3+} starts to diminish at concentrations of Eu^{3+} greater than 0.3 mol %. These discrepancies can be interpreted in terms of the restriction for the distance between Gd^{3+} and Eu^{3+} ions in the crystal. The shortest $Gd^{3+}-Eu^{3+}$ distance in the scheelite crystal is restricted to about 3.7 Å,[12] while the Gd^{3+} and Eu^{3+} ions were thought to be statistically distributed in the glass. This suggests that energy transfer from Gd^{3+} (^6P_J) to Eu^{3+} competes with the Gd^{3+} (^6P_J) to Gd^{3+} ($^8S_{7/2}$) emission process at a distance of 3.7 Å. Figure 5 shows excitation spectra of $LiGdF_4:Eu^{3+}$ observed at 613 nm (Eu^{3+}:$^5D_0 \rightarrow {}^7F_1$) when the Eu^{3+} doping concentration was changed. The Eu^{3+} ion concentration dependence of the excitation intensities measured at 275 nm (Gd^{3+}, $^6I_{7/2} \leftarrow {}^8S_{7/2}$) and at 395 nm ($Eu^{3+}$, $^5L_6 \leftarrow {}^7F_0$), where the emission was observed at 613 nm, is shown in Figure 6. The

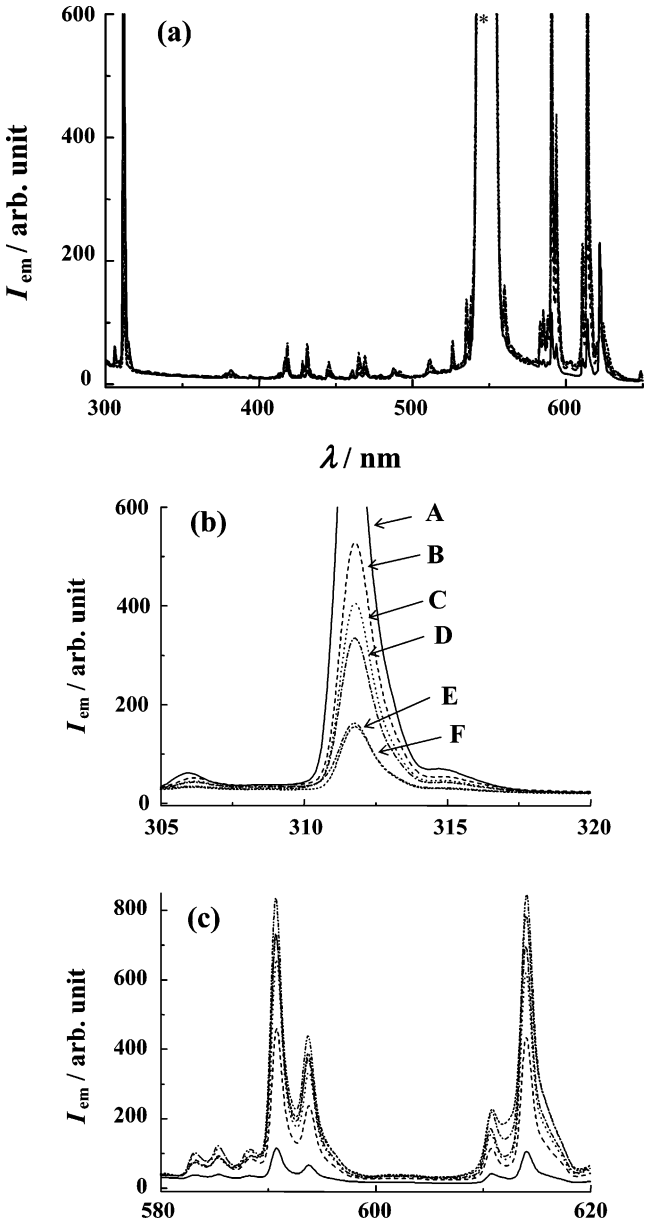

Figure 3. Eu^{3+} addition effects on the emission spectra of $LiGdF_4:Eu^{3+}$ excited at 275 nm corresponding to the $^6I_J \leftarrow {}^8S_{7/2}$ transition of Gd^{3+}. (a) 300−600 nm; (b) 305−320 nm corresponding to the $^6P_J \rightarrow {}^8S_{7/2}$ transitions of Gd^{3+}; (c) 580−620 nm corresponding to the $^5D_J \rightarrow {}^7F_J$ transitions of Eu^{3+}. (A) 0.0 mol % Eu^{3+}; (B) 0.25 mol % Eu^{3+}; (C) 0.50 mol % Eu^{3+}; (D) 1.00 mol % Eu^{3+}; (E) 5.0 mol % Eu^{3+}; (F) 10.0 mol % Eu^{3+}. The intense emission around at 550 nm noted by an asterisk is due to second-order diffraction of the 275-nm excitation light.

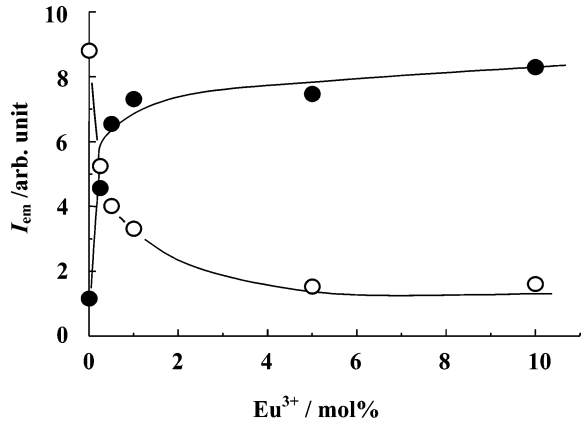

Figure 4. Codoped Eu^{3+} ion concentration dependence of the emission intensities at 313 nm (○, Gd^{3+}, $^6P_{7/2} \rightarrow {}^8S_{7/2}$) and at 591 nm (●, Eu^{3+}, $^5D_0 \rightarrow {}^7F_1$) ($\lambda_{excitation} = 275$ nm).

energy absorbed by the Gd^{3+} ions at 275 nm is efficiently transferred to Eu^{3+} ions at a low concentration of Eu^{3+}, but at 1.0 mol % Eu^{3+} doping or above, the efficiency of the energy transfer seems to saturate, while the energy absorbed directly by Eu^{3+} ions at 395 nm is effectively converted into the emission of Eu^{3+} at 613 nm. The restricted distances between an Eu^{3+} ion and a Gd^{3+} ion in the crystal seem to be reflected in the energy-transfer efficiency as discussed above.

The growth profiles of the luminescence at 313 nm (Gd^{3+}: $^6P_{7/2} \rightarrow {}^8S_{7/2}$) excited at 275 nm ($Gd^{3+}$:$^6I_J \leftarrow {}^8S_{7/2}$) are shown in Figure 7, where the rise rate seems to increase slightly from $1.3 \times 10^5\ s^{-1}$ to $2.0 \times 10^5\ s^{-1}$, although the double exponential (production−decay) fitting employed to estimate the rise rate has considerable error owing to weak intensity especially at a higher concentration of Eu^{3+}. The large spiky signals in the sub-microsecond region are considered to result from the scatter of the strong pulse laser light at 275 nm used for excitation. A similar growth behavior was also observed for Gd^{3+} emission

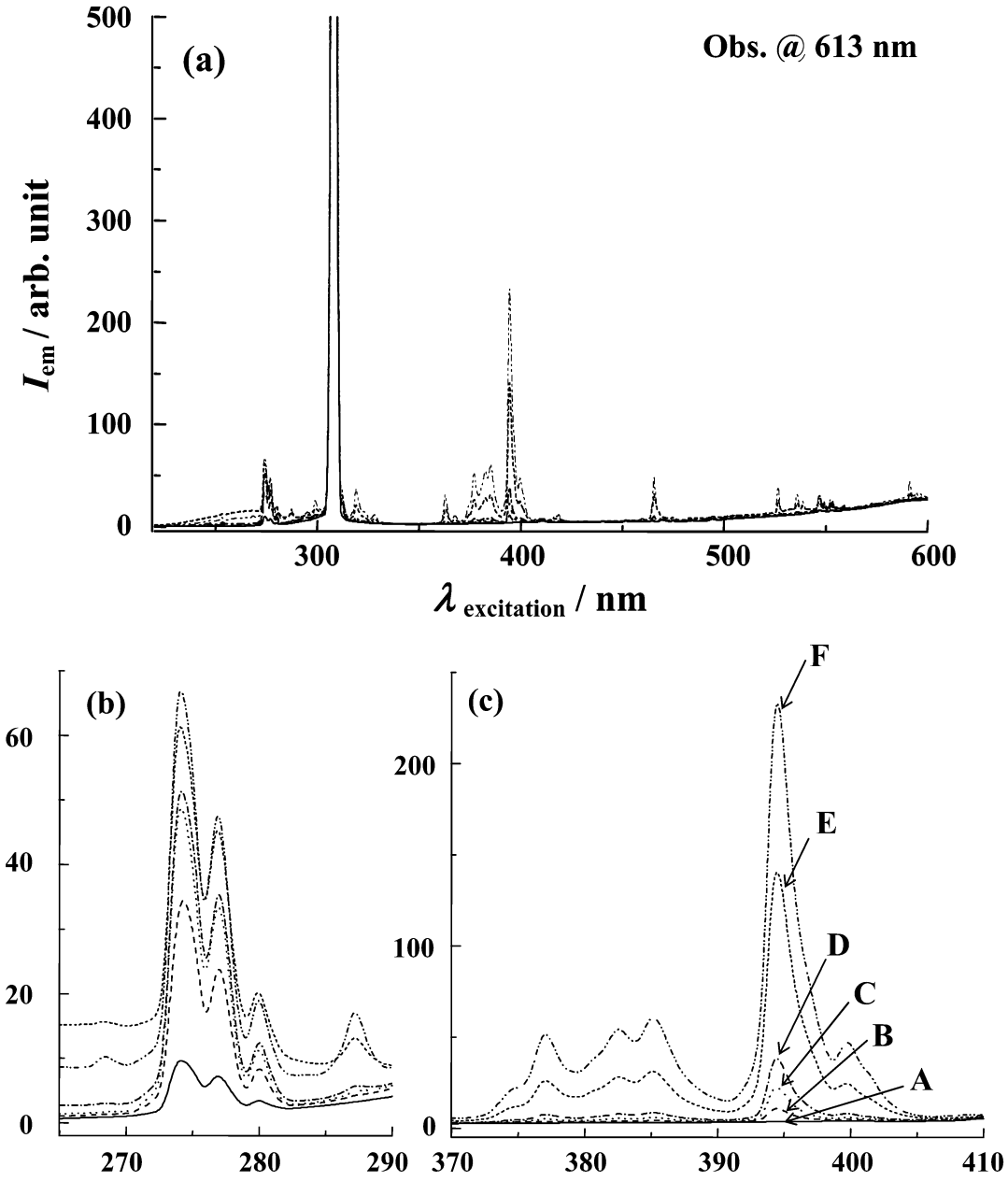

Figure 5. Excitation spectra observed at 613 nm (Eu^{3+}:$^5D_0 \rightarrow {}^7F_2$) of (a) $LiGdF_4$:Eu^{3+} in the region of 220−600 nm, (b) 265−290 nm (Gd^{3+}, $^6I_J \leftarrow {}^8S_{7/2}$), and (c) 370−410 nm ($Eu^{3+}$, $^5L_6 \leftarrow {}^7F_0$). The sample notations are the same as those in Figure 2.

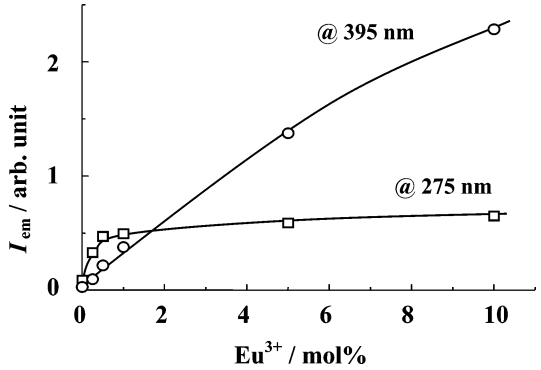

Figure 6. Codoped Eu^{3+} ion concentration dependence of the excitation intensities at 275 nm (□, Gd^{3+}, $^6I_{7/2} \leftarrow {}^8S_{7/2}$) and at 395 nm (○, Eu^{3+}, $^5L_6 \leftarrow {}^7F_0$) observed at 613 nm (Eu^{3+}:$^5D_0 \rightarrow {}^7F_2$).

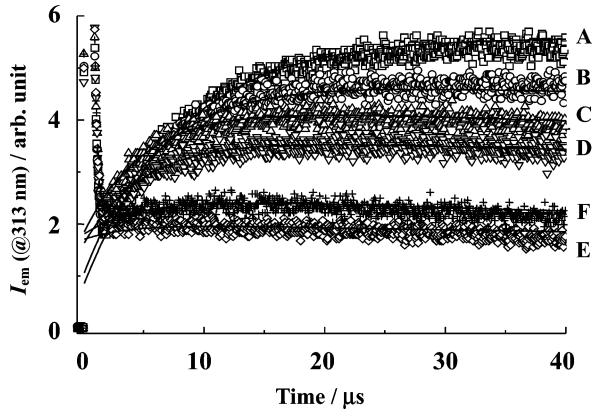

Figure 7. Eu^{3+}-addition effects on the growth curves of the transient emission at 313 nm (Gd^{3+}:$^6P_{7/2} \rightarrow {}^8S_{7/2}$) in the $LiGdF_4$:Eu^{3+} crystals excited by a 275-nm pulse (Gd^{3+}:$^6I_J \leftarrow {}^8S_{7/2}$) light. A (□), 0.00 mol % Eu^{3+} addition; B (○), 0.25 mol % Eu^{3+}; C (△), 0.50 mol % Eu^{3+}; D (▽), 1.0 mol % Eu^{3+}; E (◇), 5.0 mol % Eu^{3+}; F (+), 10.0 mol % Eu^{3+}. The intensity of each transient curve is arbitrarily magnified for clarity. The solid lines are the double exponential (production − decay) fits used to estimate the rise rates.

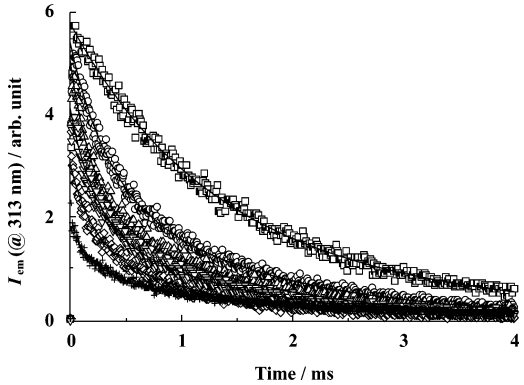

Figure 8. Eu^{3+} addition effects on the decay curves of transient emission at 313 nm (Gd^{3+}:$^6P_{7/2} \rightarrow {}^8S_{7/2}$) in the $LiGdF_4$:Eu^{3+} crystals excited by 275-nm pulsed (Gd^{3+}:$^6I_J \leftarrow {}^8S_{7/2}$) light. The concentrations of the Eu^{3+} ions are 0.00 mol % (□), 0.25 mol % (○), 0.50 mol % (△), 1.0 mol % (▽), 5.0 mol % (◇), and 10.0 mol % (+). The solid lines are the fitted curves used to estimate the decay rates. The intensity of each transient curve is arbitrarily magnified for clarity.

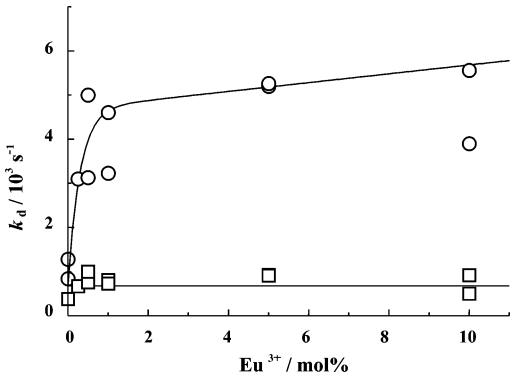

Figure 9. Dependence of the first-order decay rate of transient emission at 313 nm (Gd^{3+}:$^6P_{7/2} \rightarrow {}^8S_{7/2}$) on the Eu^{3+} concentration in the $LiGdF_4$:Eu^{3+} crystals excited by a 275-nm pulse (Gd^{3+}:$^6I_J \leftarrow {}^8S_{7/2}$) light. The symbols "○" denote the fast decay rates, and the symbols "□" do the slow decay rates.

at 313 nm in the case of soda-lime silicate glasses codoped with Gd^{3+} and Eu^{3+} ions.[15] The rise rates in the glass at 313 nm of Gd^{3+} ions are larger than those in the crystal by about 1 order of magnitude, suggesting that the intrarelaxation within the Gd^{3+} levels proceeds faster in the glass than in the crystal. One speculation for the difference between crystal and glass hosts is that the amorphous phase may support many kinds of phonon with various frequencies making relaxation to phonon modes more effective in the glasses. This is supported by the fact that the emission line has larger inhomogeneous broadening in the glass than in the crystal.[15] The dependence of the decay profile in 313-nm emission for the Eu^{3+} addition is shown in Figure 8. Two decay components were found by fitting to a two-exponential decay function ($I(t) = A \exp(-k_d^f t) + B \exp(-k_d^s t)$). One is influenced by the Eu^{3+} ions, and the other is not. The solid lines in Figure 8 are the fitted curves. The decay rates of the two components (k_d^f and k_d^s) are plotted as a function of the Eu^{3+} concentration in Figure 9. The slow decay rate seems to remain constant at about 700 s^{-1} ($\tau \approx 1.5$ ms), whereas the fast decay rate increases up to ∼1.0 mol % Eu^{3+} addition and then seems to remain constant or slightly increases until 10 mol % Eu^{3+} addition. The luminescence lifetime of the $^6P_{7/2}$ state of the Gd^{3+} ions is consistent with the reported value of (4.10 ± 0.01) ms in the borate glasses.[3] The transient behavior matches to the observation in the static emission intensity measurements (Figure 4), in which the emission intensity of Gd^{3+} at 313 nm decreases up to ∼1.0 mol % Eu^{3+} addition but does not completely disappears, whereas that of Eu^{3+} at 591 nm increases until ∼1.0 mol % Eu^{3+} addition and then remains constant until 10 mol % Eu^+ addition. Electronic energy transfer to Eu^{3+} is not efficient at higher concentrations of the Eu^{3+} ion, and about 10% of the energy absorbed by Gd^{3+} seems to remain in the form of the Gd^{3+} ion even at 10 mol % Eu^{3+}. In the $LiGdF_4$ crystal, the nearest ions of Gd^{3+} are 8 F^- located at about 2.6 Å, and the next-nearest ions are 12 (4 × Gd^{3+} and 8 × Li^+) located at about 3.7 Å. Such a restriction on the distance between Gd^{3+} and substituted Eu^{3+} is a plausible reason why the emission of Gd^{3+} at 313 nm does not completely disappear even at 10 mol % Eu^{3+} doping. The competition between emission at 313 nm and electronic energy transfer to Eu^{3+} ions in Gd^{3+} ($^6P_{7/2}$) allows a rough-order estimation for the rate of this type of electronic energy transfer of 10^4 s^{-1} at 3.7 Å distance. Nonexponential decay behavior of a donor species was observed in the phosphorescence of benzophenone (BP) adsorbed in Tb^{3+}−zeolite excited at 355 nm, where the donor was BP and the acceptor is Tb^{3+}.[16] This was interpreted in terms of the broad and inhomogeneous distributions of the acceptor within the zeolite.

Figure 10 shows the Eu^{3+}-addition effect on the luminescence decay of Eu^{3+} at 591 and 613 nm. There seems to be a slight difference in the transient behavior between the two. Though the 591 and 613 nm emissions are mainly attributed to the transitions of $^5D_0 \rightarrow {}^7F_1$ and $^5D_0 \rightarrow {}^7F_2$, respectively, other unknown transitions are also considered to be play a role. At

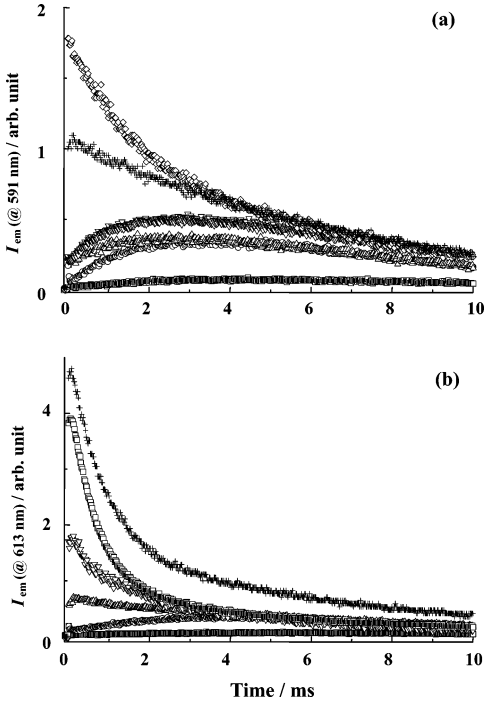

Figure 10. Eu^{3+} addition effects on the emission curves at 613 nm (Eu^{3+}:$^5D_0 \rightarrow {}^7F_2$) and at 591 nm ($Eu^{3+}$:$^5D_0 \rightarrow {}^7F_1$) in $LiGdF_4$:Eu^{3+} crystals excited by 275-nm pulse (Gd^{3+}:$^6I_J \leftarrow {}^8S_{7/2}$) light. The concentrations of the Eu^{3+} ions are 0.00 mol % (□), 0.25 mol % (○), 0.50 mol % (△), 1.0 mol % (▽), 5.0 mol % (◇), and 10.0 mol % (+).

low concentrations of Eu^{3+}, the rise times of a few ms are coincident with the fast decay at 313 nm of Gd^{3+} ($^6P_{7/2}$), showing that there is an energy transfer from Gd^{3+} ($^6P_{7/2}$) to Eu^{3+}. However, another faster energy transfer from Gd^{3+} to Eu^{3+} is thought to take an important part in the mechanism at higher Eu^{3+} concentrations because there are discrete jumps in the initial emission intensity. There are three possible schemes: direct absorption of 275 nm light by Eu^{3+} ($4f^55d^1 \leftarrow {}^7F_J$) relaxed finally to the $^5D_0$ state, resonance energy transfer from Gd^{3+} (^6I_J) to Eu^{3+} ($4f^55d^1$), and participation of fast energy transfer from Gd^{3+} ($^6B_{7/2}$) to one nearest neighbor Eu^{3+}. More careful rise-time measurements will be required for clarification of this mechanism. The tails of all the transient curves show the single-exponential decay with the same decay time of about 8 ms.

According to the experimental results, the following mechanism is proposed to describe energy relaxation and transfer in the $LiGd_{1-x}F_4$:$Eu^{3+}{}_x$ following pulsed excitation of the Gd^{3+} $^6I_{7/2}$ state

$$Gd^{3+}\,(^6I_{7/2}) \rightarrow Gd^{3+}\,(^6P_{7/2}) \quad (1)$$

$$Gd^{3+}\,(^6P_{7/2}) \rightarrow Gd^{3+}\,(^8S_{7/2}) + h\nu\,(313\ \text{nm}) \quad (2)$$

$$Gd^{3+}\,(^6P_{7/2}) + Eu^{3+}\,(^7F_J) \rightarrow Gd^{3+}\,(^8S_{7/2}) + Eu^{3+}\,(^5D_0) \quad (3)$$

$$Eu^{3+}\,(^5D_0) \rightarrow Eu^{3+}\,(^7F_1) + h\nu\,(613\ \text{nm}) \quad (4)$$

$$Eu^{3+}\,(^5D_0) \rightarrow Eu^{3+}\,(^7F_0) + h\nu\,(591\ \text{nm}) \quad (5)$$

Resonance energy transfer from Gd^{3+} ($^6I_{7/2}$) to Eu^{3+} (^7F_J) resulting in the formation of Eu^{3+} ($4f^55d^1$) was not considered here because of the relatively long distance of 3.7 Å between Gd^{3+} and Eu^{3+} in even the nearest case. The fact that the 313-nm luminescence intensities kept constant and did not decrease at the high concentration of 10 mol % Eu^{3+} (Figure 3) might support the omission of such a resonance energy transfer. At lower concentrations of Eu^{3+}, only a small portion of the Gd^{3+} ($^6P_{7/2}$) ions were quenched by energy transfer to the neighboring Eu^{3+} ions during the emission lifetime of the Gd^{3+} ($^6P_{7/2}$) ions. At higher concentration of Eu^{3+}, a large portion of the Gd^{3+} ($^6P_{7/2}$) ions were quickly quenched by energy transfer to the adjacent Eu^{3+} ions ($r(Gd^{3+} - Eu^{3+}) \approx 3.7$ Å). The rise curves of Eu^{3+} luminescence corresponding to the energy transfer in the microsecond time scale could not be observed because of the overlap with the fast formation of the Eu^{3+} ($^5D_0$) state through the intrarelaxation of the Eu^{3+} ($4f^55d^1$) produced by the direct absorption of 275-nm photons.

The high internal quantum efficiency of about 200% was reported for Gd^{3+}(donor)/Eu^{3+}(acceptor) in the $LiGdF_4$:Eu^{3+} crystalline structure upon VUV excitation in Gd^{3+} (^6G_J) by the 202-nm light.[7,9] In their paper, the internal quantum efficiency was estimated mainly from the Eu^{3+} ($^5D_0 \rightarrow {}^7F_J$) emission intensity ratios at the 600−700-nm region between the two different excitations in Gd^{3+} (^6G_J) by the 202-nm light and in Gd^{3+} (^6I_J) by the 273-nm light. Such an internal quantum efficiency (Φ) may be estimated from the kinetic rate constants such as the cross relaxation (k_{CR}) of $\{Gd^{3+}(^6G_J), Eu^{3+}(^7F_1)\} \rightarrow \{Gd^{3+}(^6P_J), Eu^{3+}(^5D_0)\}$ and the direct energy transfer (k_{DT}) from Gd^{3+} (^6G_J) to Eu^{3+} (^7F_J), assuming that nonradiative losses can be ignored and that the internal relaxation rates are small compared to k_{CR} and k_{DT}. The quantum efficiency may be determined with

$$\Phi = \frac{2k_{CR} + k_{DT}}{k_{CR} + k_{DT}} = 1 + \frac{1}{1 + (k_{DT}/k_{CR})} \quad (6)$$

Though the direct observations of those rate constants seem to be difficult because the ^6G_J state of Gd^{3+} is not emissive, the fast growth portion probably in the tens of nanoseconds region corresponding to a formation of $^5D_0$ state through a cross relaxation process and the slow growth portion in a few microseconds region corresponding to a direct relaxation process observed in the emission from $^5D_0$ state will give an useful information for the quantum cutting kinetics.

4. Conclusion

Luminescence properties and energy-transfer processes in $LiGd_{1-x}F_4$:$Eu^{3+}{}_x$ were studied by the use of a time-resolved luminescence spectroscopy with pulsed excitation at 275 nm (Gd^{3+}:$^6I_J \leftarrow {}^8S_{7/2}$). The luminescence lifetimes of Gd^{3+} ($^6P_{7/2}$) and Eu^{3+} ($^5D_0$) were estimated to be ca. 1.5 ms and ca. 8 ms, respectively. The intrarelaxation rate of the ^6I_J state to the $^6P_{7/2}$ state was also estimated to be ca. 1.3×10^5 s^{-1} from the rise rate of the luminescence at 313 nm ($\tau_{rise} \approx 8$ μs). Two decay components were observed in the 313-nm emission (Gd^{3+}:$^6P_{7/2} \rightarrow {}^8S_{7/2}$). One was influenced by Eu^{3+} addition, and the other was not. The former decay rate increased with Eu^{3+} concentration up to ~1.0 mol % and remained almost constant for further Eu^{3+} addition up to 10 mol %. The later rate corresponds to a luminescence lifetime of about 1.5 ms ($k \approx 7 \times 10^2$ s^{-1}). The observation that the absorbed energy by Gd^{3+} ions was not completely transferred to Eu^{3+} ions even at higher Eu^{3+} concentration was interpreted in terms of the fixed distance between the donor (Gd^{3+}) and the acceptor (Eu^{3+}) in the crystal.

References and Notes

(1) Person, A. D.; Peterson, G. E.; Northover, W. R. *J. Appl. Phys.* **1966**, *37*, 729.
(2) Nakazawa, E.; Shionoya, S. *J. Chem. Phys.* **1967**, *47*, 3211.

(3) Reisfeld, R.; Greenberg, E.; Velapoldi, R.; Barnett, B. *J. Chem. Phys.* **1972**, *56*, 1698.
(4) Inokuti, M.; Hirayama, F. *J. Chem. Phys.* **1965**, *43*, 1978.
(5) van Schaik, W.; van Heek, M. M. E.; Middel, W.; Blasse, G. *J. Lumin.* **1995**, *63*, 103.
(6) Wegh, R. T.; Donker, H.; Oskam, K. D.; Meijerrink, A. *Science* **1999**, *283*, 663.
(7) Wegh, R. T.; Donker, H.; Oskam, K. D.; Meijerrink, A. *J. Lumin.* **1999**, *82*, 93.
(8) Wegh, R. T.; Donker, H.; van Loef, E. V. D.; Oskam, K. D.; Meijerrink, A. *J. Lumin.* **2000**, *87*−*89*, 1017.
(9) Feldmann, C.; Justel, T.; Ronda, C. R.; Wiechert, D. U. *J. Lumin.* **2001**, *92*, 245.
(10) Ronda, C. *J. Lumin.* **2002**, *100*, 301.
(11) *CRC handbook of Chemistry and Physics*; Weast, R. C., Ed.; CRC Press: Boca Raton, FL, 1989.
(12) *Structure and properties of inorganic solids*; Galasso, F., Ed.; Pergamon Press, Ltd.: Oxford, 1970.
(13) *Solid State Chemistry: An Introduction*; Smart, L.; Moore, E., Eds.; Chapman & Hall: London, 1993.
(14) *Spectra and Energy Levels of Rare Earth Ions in Crystals*; Dieke, G. H., Ed.; Interscience Publishers: New York, 1968.
(15) Kondo, Y.; Tanaka, K.; Ota, R.; Fujii, T.; Ishikawa, Y. Submitted.
(16) Hashimoto, S.; Kirikae, S.; Tobita, S. *Phys. Chem. Chem. Phys.* **2002**, *4*, 5856.